NASA TECHNICAL MEMORANDUM

NASA TM X-52935

NASA TM X-52935



# A COMPARISON OF DWBA AND COUPLED CHANNELS IN THE 2S-1D SHELL

by R. J. Ascuitto
Yale University
New Haven, Conn.

and

Richard C. Braley and William F. Ford
Lewis Research Center
Cleveland, Ohio

TECHNICAL PAPER proposed for presentation at
American Physical Society Meeting
Stanford, California, December 28-31, 1970

# A COMPARISON OF DWBA AND COUPLED CHANNELS IN THE 2S-1D SHELL

by R. J. Ascuitto

Yale University

and Richard C. Braley and William F. Ford

National Aeronautics and Space Administration
Lewis Research Center
Cleveland, Ohio



## ABSTRACT

The success of the Hartree-Fock model in explaining the structure of nuclei in the lower half of the 2s-1d shell has created considerable interest in studies of the low-lying states of these nuclei by means such as inelastic nucleon scattering. These states are quite collective and therefore strongly excited, suggesting the need for a coupled channel analysis. This may not be necessary for all levels, however. In order to make a meaningful comparison of the coupled channel and DWBA treatments, it is necessary to adjust the DWBA optical model parameters so that both methods predict the same elastic cross section. Such a program has been carried out for the scattering of protons from $^{20}Ne$ and $^{24}Mg$, using nuclear wave functions obtained from Hartree-Fock studies. The results tend to confirm conclusions drawn in earlier investigations using a macroscopic model.[1]

## INTRODUCTION

The structure of the nuclei in the lower half of the 2s-1d shell has been described quite well by the Hartree-Fock (HF) model with projection.[2] The low-lying states of nuclei in this mass region are highly collective and hence strongly excited by inelastic nucleon scattering. One therefore expects that a coupled channel (CC) analysis will be required for all but the lowest levels, for which the customary distorted wave Born approximation (DWBA) should be adequate. This belief was investigated (for $^{20}Ne$) in an earlier publication.[3] It was found that CC and DWBA were in fairly good agreement for the excitation of the first $2^+$ state, but that DWBA was inferior for the $4^+$ and $6^+$ members of the ground state band.

In that investigation, the DWBA optical model parameters were taken to be equal to those obtained in the CC calculation. A more meaningful comparison could be made, however, if the optical model parameters used in the two methods were adjusted so that both predicted the same elastic cross section. Practically speaking, this could be managed as follows:

(1) the optimum fit to the elastic scattering is obtained using CC; (2) results of the CC calculation are then used as "experimental data" in an optical model search code; (3) the optical model parameters resulting from this search are then used in the DWBA calculation.

In this article we compare the results of the CC and DWBA methods using such a procedure, for the case of proton scattering from $^{20}$Ne and $^{24}$Mg. The target wave functions are obtained by projecting states of good angular momentum from intrinsic HF states.

## Calculation

The model space for the HF calculation consisted of a 15-state spherical basis (shell model states through the 1g shell). The harmonic oscillator length was adjusted to yield the correct value for the projected r.m.s. nuclear radius. In table I and Figures 1 and 2 the predicted radii, reduced transition rates B(E2), and energy spectra for $^{20}$Ne and $^{24}$Mg are compared with experiment.

The coupled channel treatment of inelastic scattering involves the solution of a set of coupled differential equations

$$\left[\frac{\hbar^2}{2m}\left(\frac{d^2}{dr^2} - \frac{\ell(\ell+1)}{r^2}\right) - U_{opt}(r) + E_c\right] u^{\pi I}_{cc_o}(r)$$

$$= \sum_{c'(\neq c)} \left\langle \varphi^M_{c\pi I} \middle| V \middle| \varphi^M_{c'\pi I} \right\rangle u^{\pi I}_{c'c_o}(r)$$

subject to the boundary conditions that there be outgoing waves in all channels c but incoming waves only in the elastic channel $c_o$. When the nucleon-nucleus interaction V can be expanded in irreducible tensors one finds that[4]

$$\left\langle \varphi^{M}_{c\pi I} \middle| V \middle| \varphi^{M}_{c'\pi I} \right\rangle = (2I+1)\left[\frac{2J_1+1}{2J_2+1}\right]^{1/2} \sum_{LSJ} (-1)^{L+S} V_s$$

$$\times\, U(j_2 I J J_1; J_2 j_1) \left\langle j_2 \middle\| \mathcal{J}_{LSJ} \middle\| j_1 \right\rangle \left\langle \alpha_2 J_2 \middle\| V_{LSJ}(r,\vec{A}) \middle\| \alpha_1 J_1 \right\rangle$$

where $(\alpha_1 J_1)$ and $(\alpha_2 J_2)$ refer to the initial and final nuclear states, respectively, and $j_1$ and $j_2$ to the initial and final projectile states. The reduced matrix elements of $V_{LSJ}(r,A)$ can be obtained, when the nuclear wave functions are of the HF type, by the methods discussed in reference 5.

To represent the interaction between the incoming proton and the target nucleons, we have employed the Glendenning-Veneroni potential(6)

$$V(r) = -52.0\, e^{-(r/1.85)^2} (P_{TE} + 0.6\, P_{SE})$$

The optical potential $U_{opt}(r)$ is a parametrization of the diagonal matrix elements of the effective interaction:[5]

$$U_{opt}(r) = V_{coul}(r) - V_o \rho_V(r) - i \frac{4}{a_s} W_s \rho_s(r) - V_{LS}\left(\frac{\hbar}{m_\pi c}\right)^2 \frac{\vec{\sigma}\cdot\vec{\ell}}{a_{LS} r} \rho_{LS}(r)$$

Optical model parameters for this study are given in table II (note: the CC calculation was made using 12 partial waves).

## RESULTS

Comparisons of the elastic scattering cross sections predicted by CC and DWBA are presented in Figures 3 and 4. The DWBA optical model parameters (see table II) were obtained using the procedure outlined in the Introduction (the CC results are the "data" in Figs. 3 and 4). Except for the strength of the absorptive potential (which must be larger in a DWBA calculation to compensate for the missing channels), the parameters change only slightly for $^{20}$Ne. For $^{24}$Mg it proves necessary to make substantial

changes in other parameters as well.

Figures 5 and 6 show the various proton scattering cross sections for $^{20}$Ne and $^{24}$Mg, respectively, as predicted by both the CC and DWBA methods. By construction, the elastic cross sections predicted by each are nearly identical; the $2^+$ cross sections are also in good agreement. For both nuclei, however, predicted values of cross sections for exciting the higher levels depend strongly on which method is used.

Figures 7 and 8 compare the CC cross sections to the experimental data.[6] The inelastic cross sections invariably underestimate the data, although for the $2^+$ levels the discrepancy is not large.

Figure 9 gives the result of a macroscopic calculation[1] for proton scattering on $^{20}$Ne. It is evident that the $4^+$ cross section cannot be fit unless the deformation parameter $\beta_4$ is given a positive value of the order of $\beta_2^2$. This implies that the direct excitation $(0^+ \rightarrow 4^+)$ is roughly as effective as the indirect excitation $(0^+ \rightarrow 2^+ \rightarrow 4^+)$ in contributing to the $4^+$ cross section. The DWBA calculation includes only the former, and so may be expected to underestimate the CC result by about a factor of 2; this is borne out by the $4^+$ cross sections displayed in Figure 5.

A somewhat different situation prevails in the case of $^{24}$Mg. Here the best macroscopic model fits to the data, shown in Figure 10, are achieved for deformation parameter values such that $|\beta_4| \ll \beta_2^2$. Consequently one would expect that the DWBA calculation of the $4^+$ cross section, which treats only the direct excitation, would considerably underestimate the CC result. This indeed occurs, as may be seen in Figure 6.

## DISCUSSION

The primary object of this investigation has been to study the reliability of DWBA-predicted cross sections for the light deformed nuclei in the 2s-1d shell, using a microscopic model to describe the nuclear states. The DWBA appears to be quite adequate for excitation of the $2^+$ level in both $^{20}$Ne and $^{24}$Mg, but cross sections for the higher-lying levels are altered significantly by the CC calculation. In particular, the DWBA and CC predictions for the $4^+$ cross section in $^{24}$Mg are very different, which can be understood in terms of the deformation parameters used by the macroscopic model.

As a byproduct of this investigation, however, we have dramatic evidence of the reliability of the HF model of the nucleus. In one sense, the use of a macroscopic model in analyzing nuclear reactions is simply to parametrize the scattering data in terms of gross features of the

nucleus--namely its quadrupole and hexadecapole moments, measured by the parameters $\beta_2$ and $\beta_4$. Thus, when calculations of scattering cross sections performed using HF nuclear wave functions exhibit the same behavior as calculations using the macroscopic model, one can infer that the moments, or shape, of the nucleus must be quite well described by the HF model. Further evidence of this is provided by the nuclear moments in the intrinsic state, which are listed in table III: the smallness of the $^{24}$Mg hexadecapole moment is striking. These are encouraging indications that the HF wave function, which is obtained entirely from energy considerations and with no regard to the scattering data, is providing at least qualitatively the sort of shape variation which is necessary to explain the inelastic cross sections.

## REFERENCES


1. R. de Swiniarski, C. Glashausser, D. L. Hendrie, J. Sherman, A. D. Bacher and E. A. McClatchie, Phys. Rev. Letters 23, 317 (1969), and private communication.

2. M. R. Gunye, Nucl. Phys. A128, 457 (1969).
   B. Giraud and P. Sauer, Phys. Letters 30B, 218 (1969).
   W. F. Ford, R. C. Braley, and J. Bar-Touv, A Study of the Hartree-Fock Model Space for Light Deformed Nuclei. NASA TN (to be published).

3. R. J. Ascuitto, W. F. Ford, R. C. Braley and J. Bar-Touv, Bull. Am. Phys. Soc. 15, 502 (1970).

4. N. K. Glendenning, Nucl. Phys. A117, 49 (1968).

5. R. C. Braley and W. F. Ford, Phys. Rev. 182, 1174 (1969).

6. N. K. Glendenning and M. Veneroni, Phys. Rev. 144, 839 (1966).

TABLE I. - COMPARISON OF PREDICTED AND EXPERIMENTAL RADII AND E2 RATES FOR (a) $^{20}Ne$ and (b) $^{24}Mg$

| (a) $^{20}Ne$ | | | | |
|---|---|---|---|---|
| | $\langle R^2 \rangle^{1/2}$, fm. | B(E2; $0^+ - 2^+$) $e^2 \cdot fm^4$ | B(E2; $2^+ - 4^+$) $e^2 \cdot fm^4$ | B(E2; $4^+ - 6^+$) $e^2 \cdot fm^4$ |
| Predicted | 2.78 | 204 | 103 | 90 |
| Experiment | 2.79 | $286 \pm 15$ | $89 \pm 9$ | $129 \pm 13$ |

| (b) $^{24}Mg$ | | | |
|---|---|---|---|
| | $\langle R^2 \rangle^{1/2}$ fm. | B(E2; $0^+ - 2^+$) $e^2 \cdot fm^4$ | B(E2; $2^+ - 4^+$) $e^2 \cdot fm^4$ |
| Predicted | 3.04 | 374 | 191 |
| Experiment | $3.02 \pm 0.03$ | $436 \pm 46$ | $133 \pm 13$ |

TABLE II. - COMPARISON OF CC AND DWBA OPTICAL MODEL PARAMETERS FOR $^{20}Ne$ AND $^{24}Mg$

| | $V_o$, MeV | $W_s$ MeV | $V_{LS}$ MeV | $r_o$ fm | $r_s$ fm | $r_{LS}$ fm | $a_o$ fm | $a_s$ fm | $a_{LS}$ fm |
|---|---|---|---|---|---|---|---|---|---|
| $^{20}Ne$, CC | 55.4 | 7.05 | 3.58 | 1.05 | 1.265 | 0.96 | 0.73 | 0.61 | 0.33 |
| $^{20}Ne$, DWBA | 54.5 | 8.12 | 3.58 | 1.073 | 1.251 | 0.96 | 0.713 | 0.61 | 0.33 |
| $^{24}Mg$, CC | 49.1 | 6.56 | 5.29 | 1.174 | 1.19 | 1.06 | 0.736 | 0.562 | 0.546 |
| $^{24}Mg$, DWBA | 46.1 | 8.30 | 5.29 | 1.241 | 1.163 | 1.06 | 0.665 | 0.552 | 0.546 |

TABLE III. - MASS QUADRUPOLE ($Q_2$) AND HEXADECAPOLE ($Q_4$) MOMENTS FOR $^{20}Ne$ AND $^{24}Mg$

| | $Q_2$, $fm^2$ | $Q_4$, $fm^4$ |
|---|---|---|
| $^{20}Ne$ | 36.32 | 241.18 |
| $^{24}Mg$ | 43.19 | 53.77 |

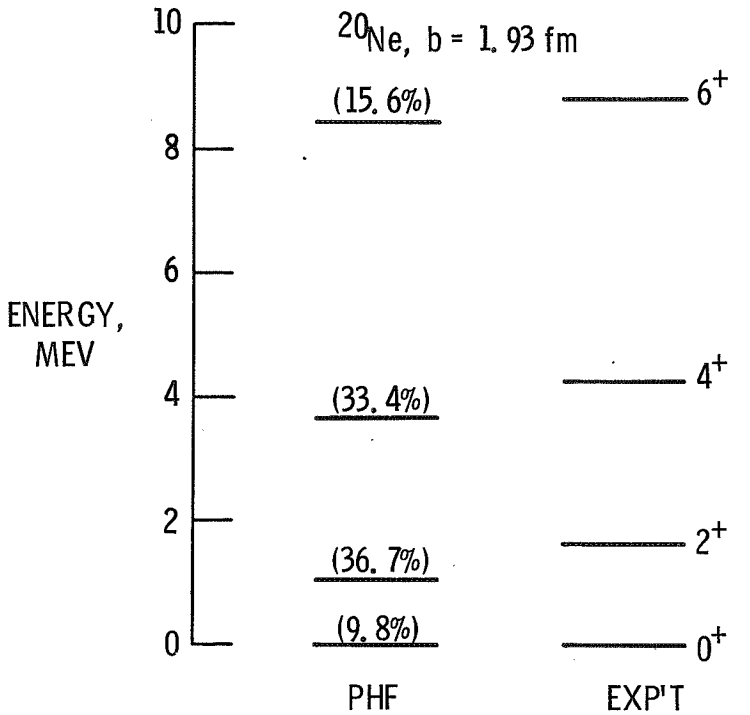


Figure 1.

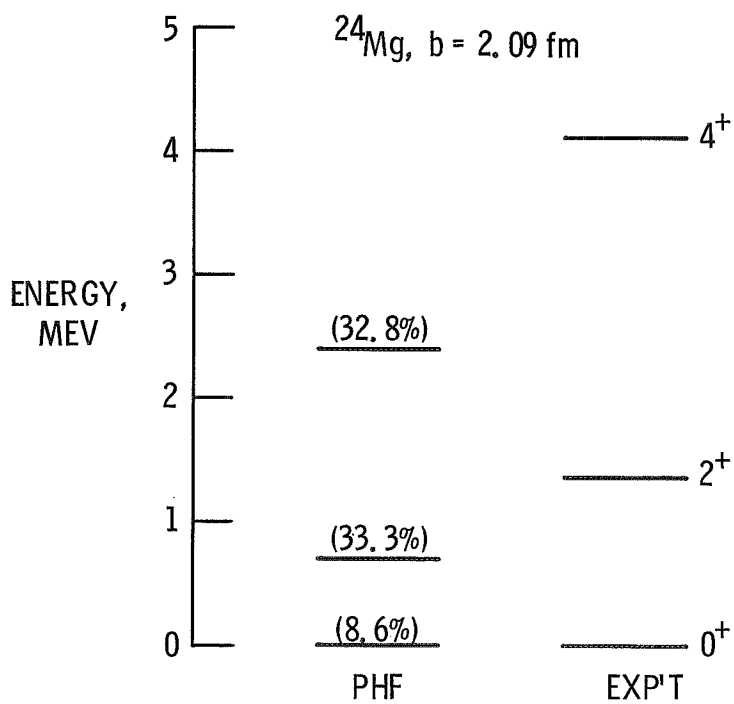


Figure 2.

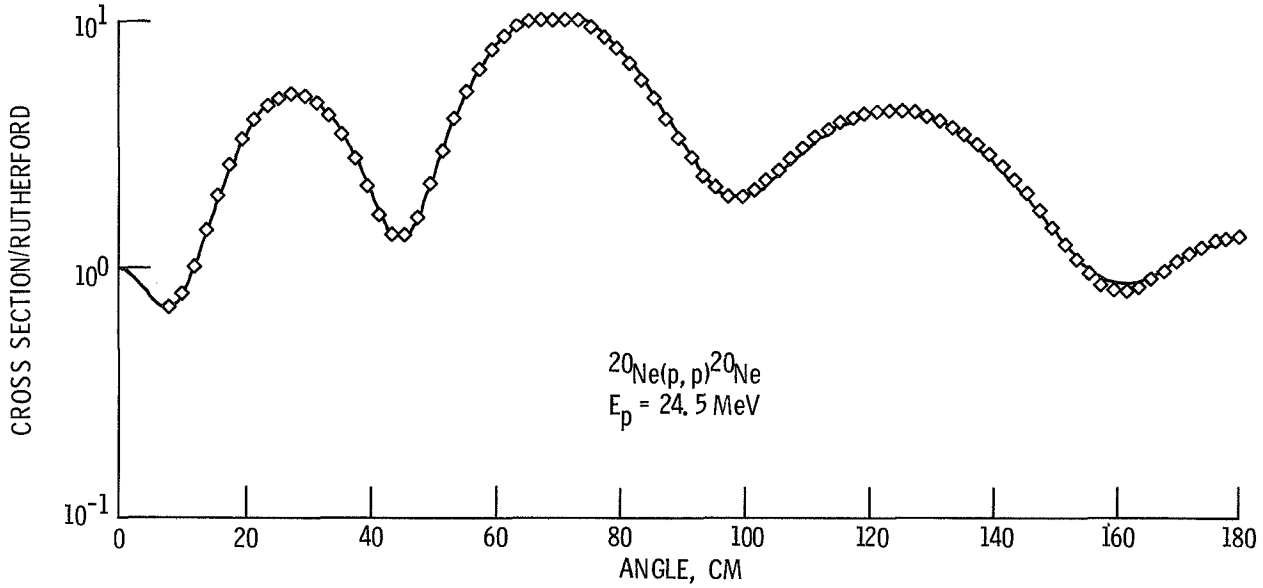


Figure 3.

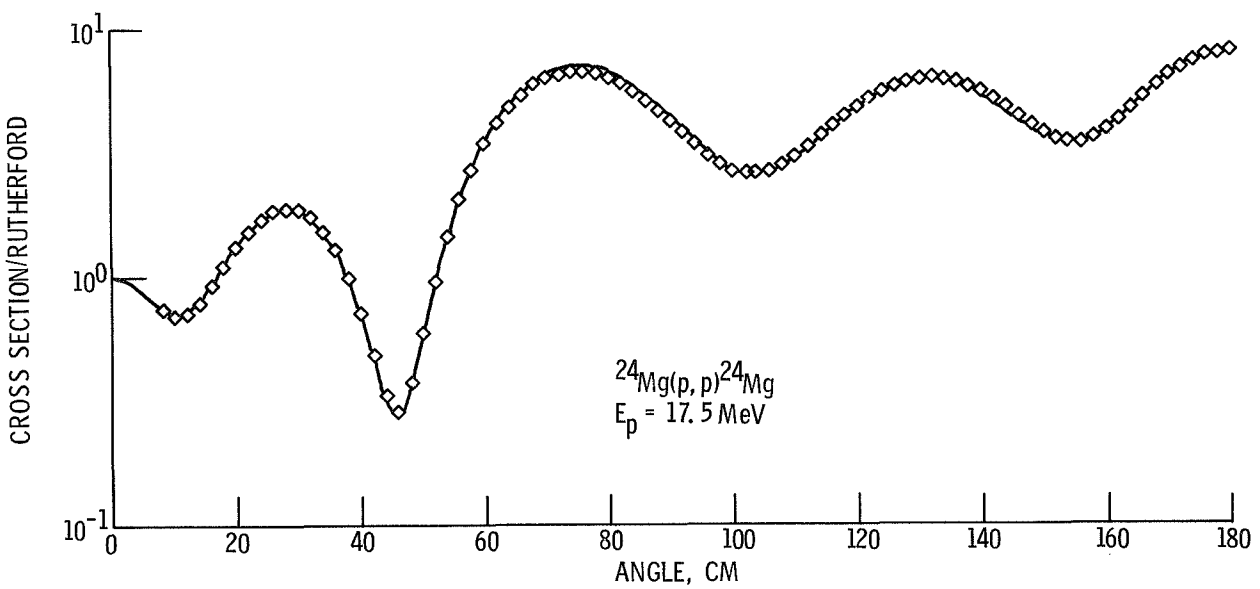


Figure 4.

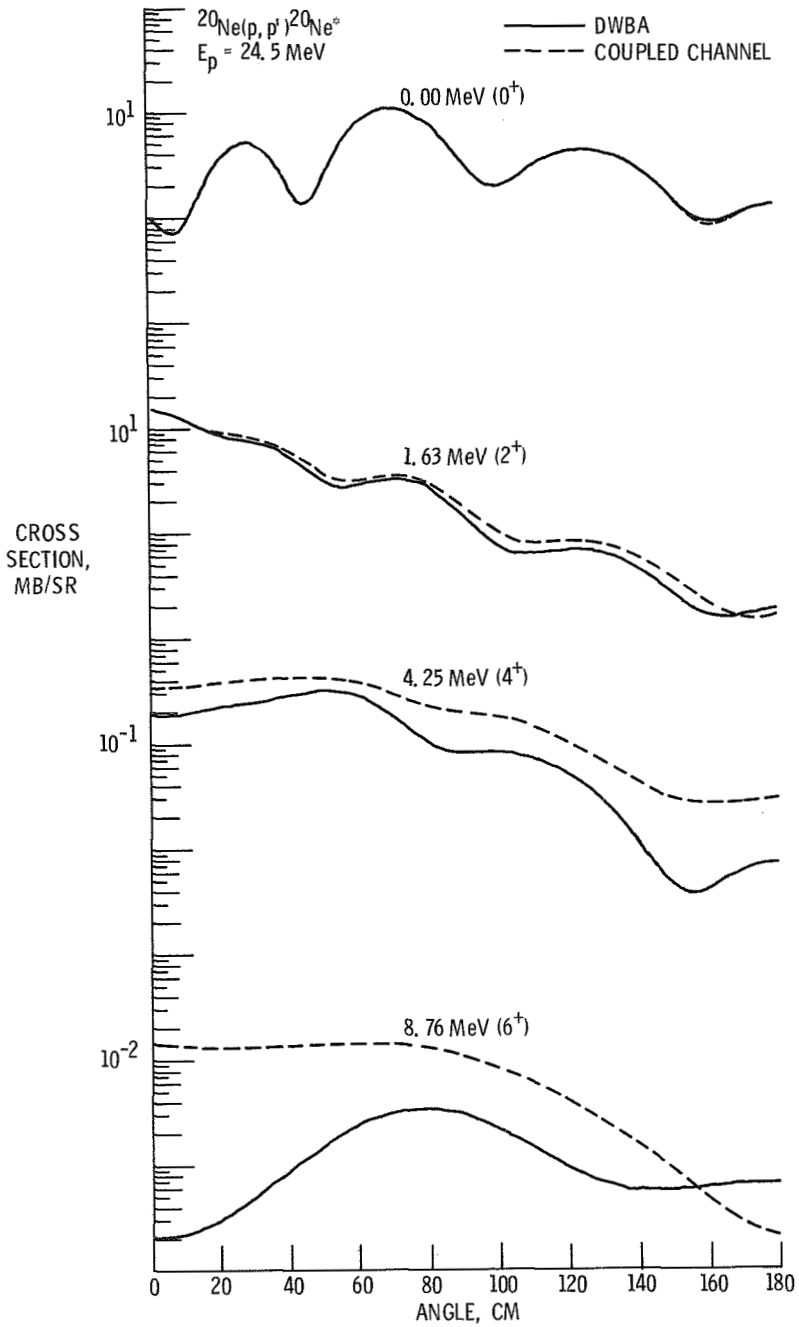


Figure 5.

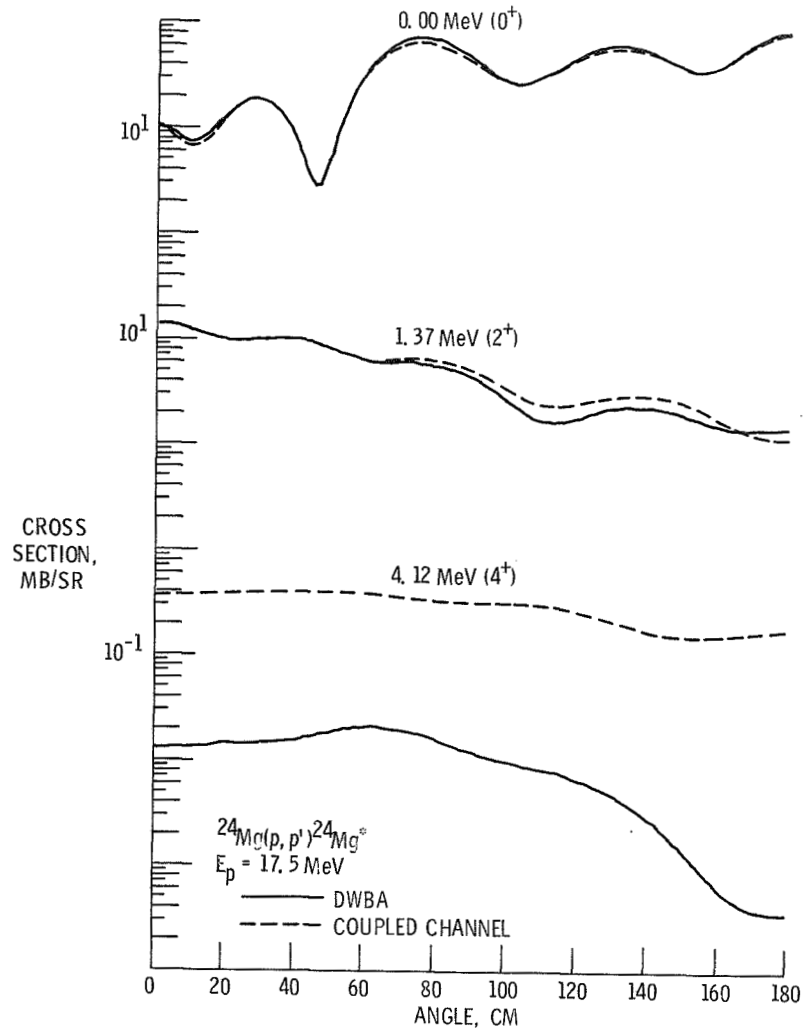


Figure 6.

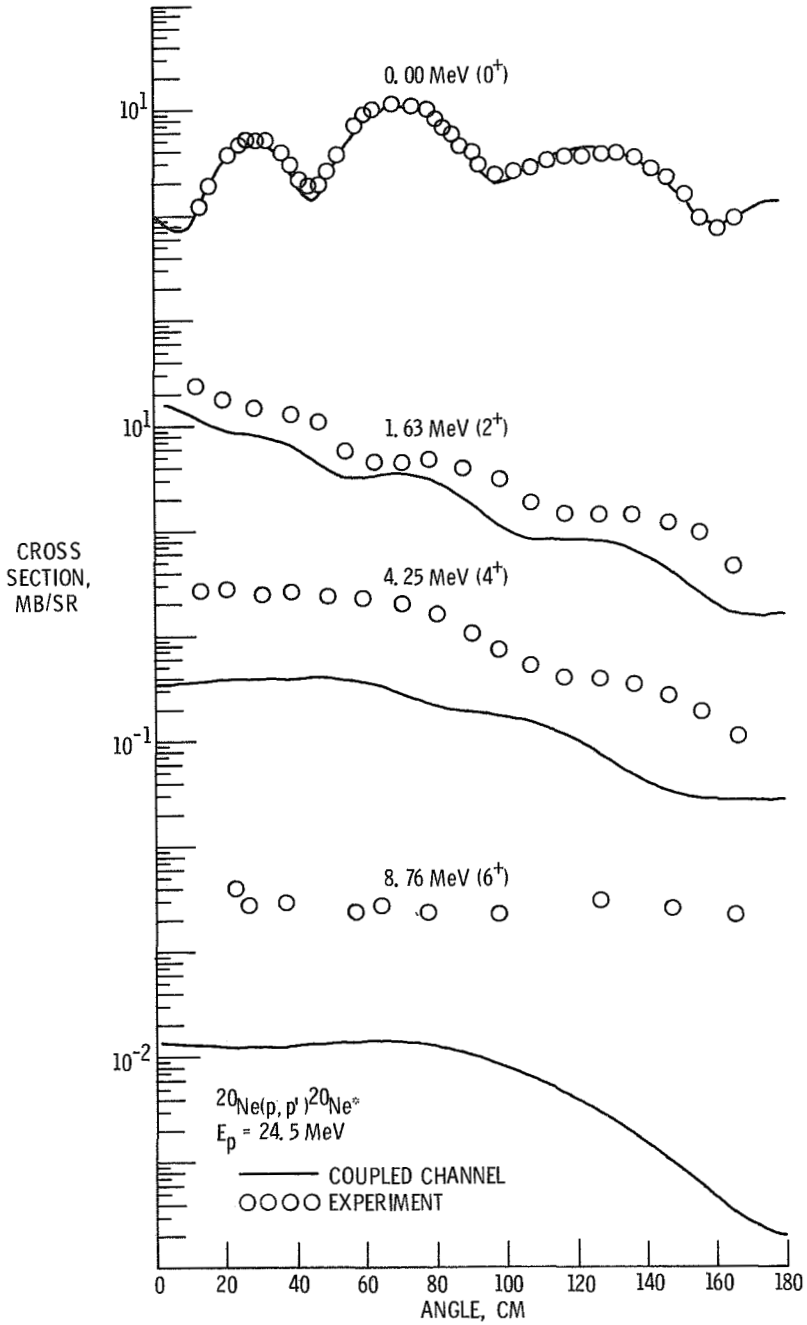


Figure 7.

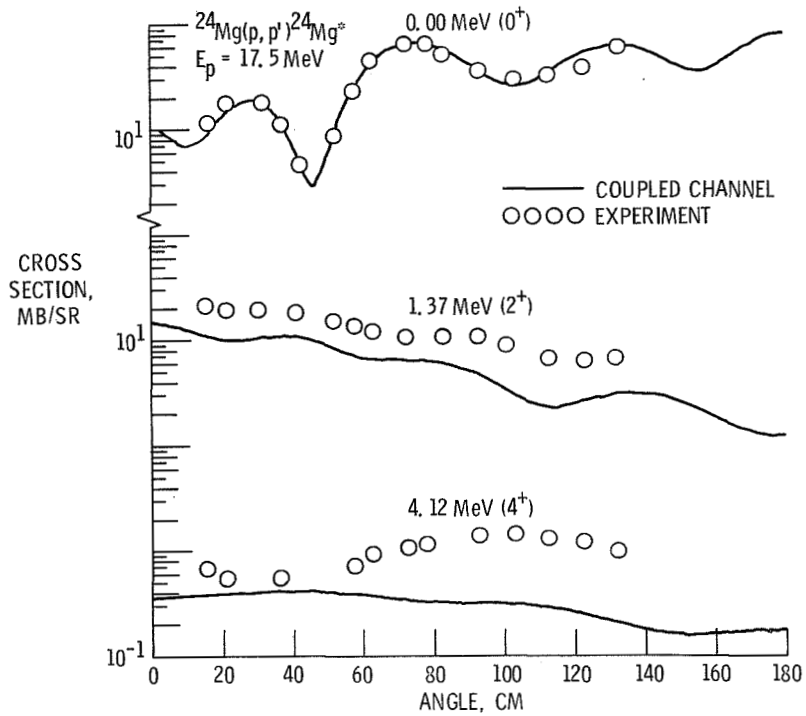


Figure 8.

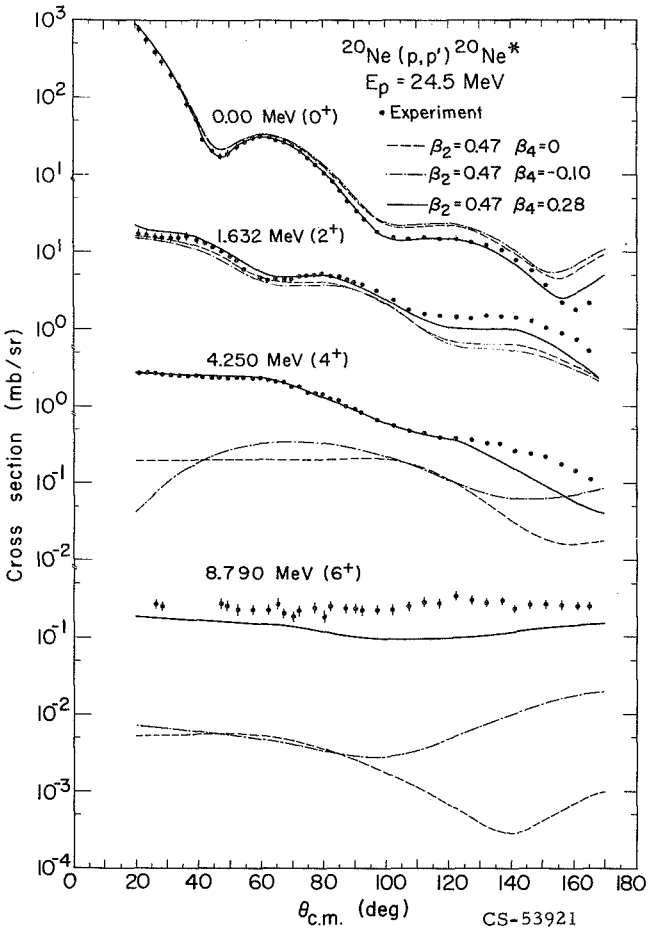


Figure 9.

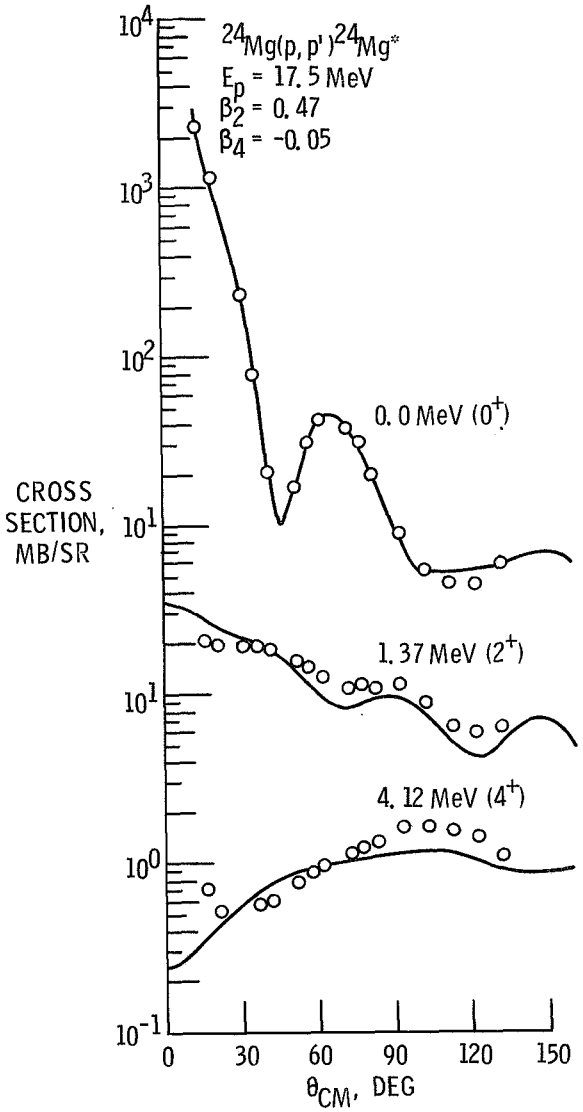


Figure 10.